Methylcyclohexane Ring-Contraction: A Sensitive Solid Acidity and Shape Selectivity Probe Reaction[†]

Gary B. McVicker,* Owen C. Feeley, John J. Ziemiak, David E. W. Vaughan, Karl C. Strohmaier, Wayne R. Kliewer, and Daniel P. Leta

Corporate Strategic Research Laboratories, ExxonMobil Research and Engineering Company,
1545 Route 22 East, Annandale, New Jersey 08801

Received: March 9, 2004

In this paper we describe the utility of an acid-catalyzed isomerization reaction, specifically, ring-contraction of methylcyclohexane to an isomeric mixture of alkylcyclopentanes as a tool for characterizing the acidic properties of a wide range of platinum-loaded solid acids. Methylcyclohexane isomerization is particularly useful as a solid acidity probe reaction since it is a simple molecule containing one six-membered ring and a single methyl group substituent. As a solid acidity probe molecule methylcyclohexane has a number of advantages over cyclohexane. Ring-contraction of cyclohexane produces a single product, methlycyclopentane. Methylcyclohexane ring-contraction, in contrast, yields a richer and thus more informative product mixture including ethylcyclopentane, and five isomeric dimethylcyclopentanes. For the first time it will be shown that variations in the three primary descriptors of solid acids, acid site density, acid site strength, and shape selectivity, within a wide range of amorphous and crystalline solid acids can be simultaneously ranked using a single component probe reaction, namely, methylcyclohexane ring-contraction.

1. Introduction

Solid acid catalysts are extensively used by the petroleum industry for the production of motor fuels and a wide range of petrochemicals.[1,2] Since a large number of hydrocarbon conversion reactions are involved, it is important to establish reliable test protocols that correlate the physical and compositional properties of solid acids with the acidity requirements of the specific reaction being catalyzed. Well-designed probe reactions can identify subtle differences in both metal and acid functions, aid process condition optimization, and provide insight into catalyst activation, deactivation, and regeneration processes. In this paper we describe the use of a simple solid acid promoted hydrocarbon conversion reaction, namely, ring-contraction of methylcyclohexane (MCH) to a mixture of ethylcyclopentane (ECP) and dimethylcyclopentane (DMCP) isomers, as a probe reaction for characterizing the acidity parameters of a wide range of platinum-loaded solid acids. MCH ring-contraction rates and product patterns can be used to appraise not only the relative number and relative strength of acid sites in both amorphous and crystalline solid acids, but can additionally evaluate subtle shape selectivity differences in zeolites and microporous materials. Figure 1 summarizes the relationships observed among MCH conversions and product selectivities and the three key acidity parameters attributed to solid acids.

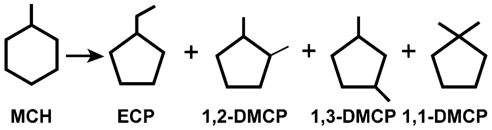

Figure 1. MCH ring-contraction patterns discern three key solid acidity characteristics. (1) Overall conversions, under a given set of reaction conditions, are proportional to the number of effective acid sites for both amorphous and crystalline solid acids. (2) ECP selectivities, at a particular conversion, reflect relative differences in acid strengths. (3) The *trans*-1,2-DMCP/*trans*-1,3-DMCP product ratio discriminates product shape selectivity differences in microporous and zeolitic materials.

First, the relative number of effective acid sites can be ascertained by comparing overall ring-contraction activities under a given set of reaction conditions. For example, if catalyst “A” under a specific set of reaction conditions selectively converted 50% of MCH to ring-contraction products, while catalyst “B” under identical conditions selectively converted only 25% of MCH catalyst it is reasonable to suggest that catalyst “A” contains twice as many effective acid sites as catalyst “B”. Second, relative strengths of solid acids can be estimated by comparing selectivity differences shown toward a particular ring-contraction product. At low MCH conversion levels (10−20%) weaker acid strength solid acids typically exhibit >70% selectivities toward the nonbranching ECP isomer while stronger acid strength solid acids produce larger quantities (50−70%) of the doubly branched DMCP isomers. The relative ease of forming ECP is rationalized as resulting from the facile rearrangement of a tertiary carbocation.[3] Formation of DMCP isomers, which demands stronger acid sites and furthermore cannot be formed by a tertiary carbocation route, is assumed to occur via parallel, nonclassical carbocation (ionic) routes utilizing protonated cyclopropane transition states (see Figure 2).[4] Postulated carbocation transition states for the various MCH ring-contraction products are listed in the order of decreasing stabilities.[5]

Increasing acid strength should enhance the extent to which the individual DMCP isomer concentrations approach equilibrium.[6] Based upon this postulate, ECP selectivity, at a given MCH conversion, can be used as a relative measure of acid strength. Last, the *trans*-1,2-DMCP/*trans*-1,3-DMCP isomer ratio was found to vary between 0.1 and 2.4 over a large number

---

[†] Part of the special issue “Michel Boudart Festschrift”.

* To whom correspondence should be addressed. E-mail: gary.b.mcvicker@exxonmobil.com.

10.1021/jp040205k CCC: $30.25

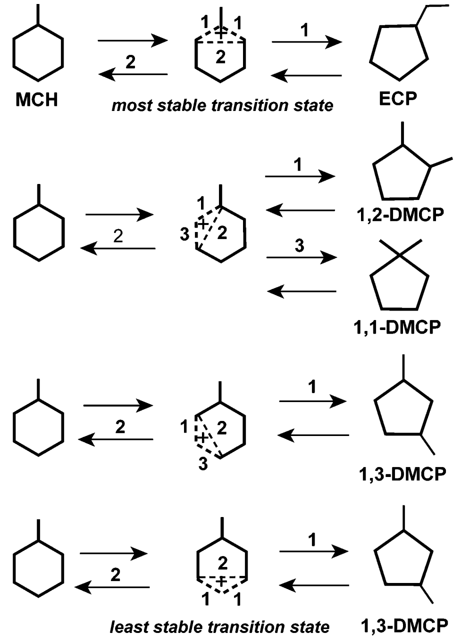

Figure 2. Possible nonclassical carbocation (ionic) routes for the ring-contraction of methylcyclohexane to ethylcyclopentane and isomeric dimethylcyclopentanes.

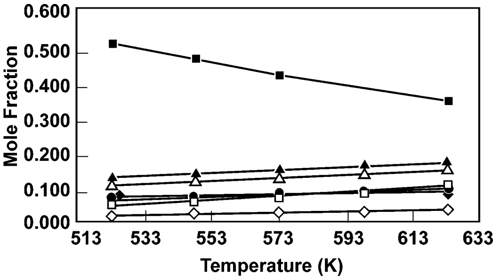

Figure 3. Equilibrium distribution of MCH ring-contraction products. Symbol codes: ■ MCH, □ ECP, ◆1,1-DMCP, ◇ *cis*-1,2-DMCP, ▲ *trans*-1,2-DMCP, △ *cis*-1,3-DMCP, and ● *trans*-1,3-DMCP.

of representative solid acids. The substantial variability exhibited by this ratio is consistent with a product shape selectivity dependence resulting from differences in the transport capabilities of the 1,2- and 1,3-DMCP isomers. The less bulky 1,3-DMCP isomer would likely experience a smaller transport inhibition than the bulkier 1,2-DMCP isomer through the intracrystalline channels and pore mouths of 10- and 12-ring zeolites and microporous materials.[7] Ten-ring zeolitic and microporous materials typically display *trans*-1,2-DMCP/*trans*-1,3-DMCP ratios in the 0.1 to 0.5 range, while larger pore size 12-ring zeolites and amorphous solid acids exhibit much higher values for this isomer ratio, ranging from 1.2 to 2.4. Over the rather broad temperature range utilized throughout these studies the equilibrium value for the *trans*-1,2-DMCP/*trans*-1,3-DMCP ratio remains near 1.8−1.9 (see Figure 3).

2. Experimental Section

2.1. Catalysts. Metal-loaded catalysts were prepared by conventional incipient wetness impregnation of well-characterized amorphous and crystalline zeolitic and microporous acidic supports with a standardized platinum solution (0.10 g Pt/cm^3). Representative solid acids employed in these studies include halided-Al_2O_3, amorphous $SiO_2-Al_2O_3$, and crystalline zeolitic and microporous materials including Beta, MOR, ZSM-5, SAPO-11, ZSM-22, EU-1, ZSM-23, CLINO, and high-silica FAU (USY)-materials. Those interested in obtaining detailed structural information on the various zeolitic and microporous materials employed in these studies should consult ref 8. Metal analyses were in all cases in good agreement with nominal value of 0.5 wt % Pt. Routine X-ray diffraction measurements on zeolitic and microporous materials yield sample crystallinity and lattice parameter information that in the case of zeolites provide an estimate of the Si/Al molar ratio. Solid-state MAS NMR measurements furnished a direct measure of framework Al content, while elemental analyses supplied bulk Si/Al values. Additional catalyst preparation and characterization particulars can be found in refs 9−11.

TABLE 1: MCH Conversion Patterns Over Solid Acids are Well Behaved

catalyst[a]	g	WHSV	rates (g/h/g)[b] total	RC	ECP	% ECP selectivity
ZSM-22	0.25	62	1.39	1.33	0.82	62
	1.5	10	1.38	1.28	0.62	48
$SiO_2-Al_2O_2$[c]	0.25	62	0.75	0.73	0.38	52
	2.0	8	0.70	0.70	0.34	49
	equlibrium value					*10*

[a] Catalysts contain 0.5 wt % Pt. [b] Conditions: 553 K, 1475 kPa, 20 cm^3 MCH/h, H_2/MCH = 5, MCH conversions <15%, RC = ring-contraction rate. [c] Amorphous.

2.2. Reactor System. MCH ring-contraction experiments were carried out in a 25-cm^3 stainless steel, fixed-bed, downflow reactor capable of operating pressures to 5500 kPa and temperatures to 823 K. The reactor was heated by a fluidized sand bath, which provided isothermal operation throughout the reactor zone. Neat, high-purity MCH was fed without pretreatment to the reactor by a dual-barrel Ruska feed pump. The upper portion of the reactor contained inert mullite beads, which served as a preheat zone and also minimized dead space volume. Total reactor effluent was analyzed online by a Wasson engineered GC system equipped with a 60-m capillary column having a methylsilicone stationary phase. All reaction products, ranging in molecular weight from methane through the isomeric xylenes, were verified by supplementary GC/MS analyses. The reactor was charged with 0.25−2.0 g of catalyst. Catalysts were prereduced at 773 K under a flow of 500 cm^3/min of H_2 under 1400−2900 kPa total pressure. Initial reaction temperatures were determined by the reactivity of the particular solid acid employed. Liquid MCH was fed to the reactor at 10−20 cm^3/h. The H_2 flow was adjusted to provide the desired H_2/MCH mole ratio. After steady-state conversion was achieved the reaction temperature was increased by 10−25 K increments. The reaction temperature was routinely returned to an intermediate value to establish the extent of catalyst deactivation. No significant deactivation was noted in any of the solid acid systems tested.

3. Results and Discussion

3.1. MCH Ring-Contraction is a Well-Behaved Reaction. MCH conversion patterns over both amorphous and crystalline zeolitic and microporous solid acids are reproducible and readily measured by conventional GC techniques. To illustrate the reliability of the ring-contraction reaction, overall MCH rates exhibited by ZSM-22, a crystalline 10-ring zeolite, and an amorphous $SiO_2-Al_2O_3$ solid acid were found to remain constant over a 6−8-fold change in weight hourly space velocity (Table 1).

Selectivities toward ring-contraction (defined as RC rate/total rate) remain above 90% over the conditions employed. Selec-

TABLE 2: MCH Conversion Patterns are not Strongly Dependent Upon Platinum Dispersion

			wt % @ 593 K[c]			ECP selectivity
catalyst[a]	Si/Al	H/Pt[b]	conv.	RC	cracking	@ 10% conv.
ZSM-22	27	0.20	22.9	22.1	0.48	67
ZSM-22	27	0.67	19.2	18.2	0.65	62
EU-1	25	0.09	42.5	38.0	4.0	23
EU-1	25	0.90	37.8	32.9	4.5	22
		equilibrium value				*8−11*

[a] Catalysts contain 0.5 wt % Pt. [b] H/Pt determined by hydrogen chemisorption. [c] Conditions: 473−613 K, 1475 kPa, WHSV = 31, H_2/MCH = 5.0, RC = ring-contraction.

TABLE 3: Relative MCH Ring-Contraction Rates can be Used to Estimate Acid Site Densities[a]

catalyst 0.5% Pt	Si/Al	ring-contraction rate[b]	relative number of acid sites
Pt/Al_2O_3		0.05	1.0
Pt/SAPO-11	0.05	1.0	20
Pt/SiO_2−Al_2O_3	3.4	1.4	28
Pt/1.5%F−Al_2O_3		3.9	78
Pt/USY	37	25	500
Pt/USY	8.3	105	2100
Pt/USY	5.1	132	2640
Pt/Beta	15	126	2520

[a] Conditions: WHSV = 31, H_2/MCH = 5, 2850 kPa, 548−598 K. [b] Rates in mol/h/g × 1000, at 548 K.

tivities toward the ECP isomer decreased, as expected, with increasing conversion. Side reactions such as acid site cracking and metal site dehydrogenation were minimized by the choice of reaction conditions. Acid site cracking becomes important only at higher temperatures and then only with the use of more strongly acidic catalysts. Dehydrogenation of MCH to toluene, as well as to olefins, is limited by the relatively high hydrogen partial pressure (1230 kPa) and low temperatures used. Higher hydrogen partial pressures also significantly reduce catalyst deactivation rates. During the course of these studies it was observed that ring-contraction of MCH over a wide range of platinum-loaded solid acids was not highly dependent upon the activity of the platinum component. As shown in Table 2 platinum dispersions differing by a factor of 10 had only a limited effect on the ring-contraction and cracking activities and ECP selectivities of ZSM-22 and EU-1 based hydroisomerization catalysts. This observation suggests that only small quantities of platinum are required to generate equilibrium quantities of olefins, which in turn are readily transformed into ionic intermediates on the acidic ZSM-22 and EU-1 supports.[12]

3.2. Relative MCH Ring-Contraction Rates can be used to Estimate Acid Site Densities. MCH ring-contraction rates for a wide variety of solid acids are compared in Table 3. Ring-contraction rates normalized to the least active catalyst Pt/Al_2O_3 catalyst provide a relative scale of acid site densities that spans 3 orders of magnitude. Ring-contraction rates for Al_2O_3 based catalysts are increased 80-fold upon addition of 1.5 wt % fluorine, indicating a substantial increase in the number of effective acid sites. This large increase in the number of effective acid sites suggests that upon fluoridation initially inactive Al_2O_3 hydroxyl groups are transformed, presumably by electron induction effects, into Brønsted acid sites of sufficient strength to more efficiently catalyze ring-contraction.[13] For a series of ultrastable faujasites (USYs) the relative number of effective acid sites increases smoothly with decreasing zeolite Si/Al ratios. The most active USY (Si/Al = 5.1) catalyst studied is at least 2600 times more active than Al_2O_3. A Beta zeolite having a significantly lower framework Al content, Si/Al = 15, displayed an activity comparable to that of the most active USY (Si/Al = 5.1) catalyst. This suggests that at comparable framework Al contents the acid sites present in a Beta zeolite are likely stronger and therefore more effective for MCH ring-contraction than those of USY. Arrhenius plots for a variety of both amorphous and crystalline solid acids (see Figure 4) established that apparent activation energies associated with MCH ring-contraction fall within the range of 28−32 kcal/mol (117−134 kJ/mol). This is an important observation since a common activation energy allows catalysts with markedly differing activities to be compared (ranked) at a given temperature.

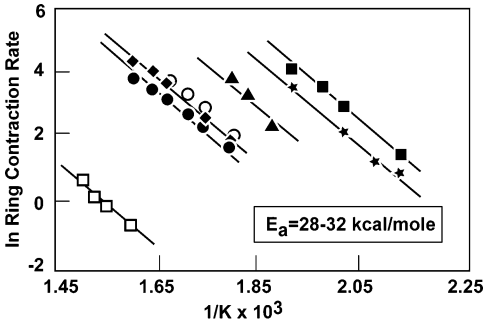

Figure 4. Arrhenius plots for MCH ring-contraction over representative amorphous and crystalline solid acids. Run conditions: 2850 kPa, H_2/MCH = 5, WHSV = 31, catalysts contain 0.5% Pt. Symbol codes: ☐ Pt/Al_2O_3, ● Pt/SAPO-11, ◆ Pt/SiO_2−Al_2O_3, ○ Pt/USY (95), ▲ Pt/USY (40), ☆ Pt/USY (12), ■ Pt/USY (5.1); (number in parentheses) = Si/Al mole ratio.

3.3. Acid Strength Information can be Abstracted from Ring-Contraction Product Patterns. Thermodynamics favor five-membered rings over six-membered rings at temperatures typically used in petroleum processing.[14] As shown in Figure 3, five-membered ring isomers become favorable above 500 K. Figure 3 also shows that ECP and 1,1-DMCP are less favored than the combined dibranched *cis*- and *trans*-1,2-DMCP and *cis*- and *trans*-1,3-DMCP isomers. As described in section 3.2., overall MCH ring-contraction rates are a reliable gauge of the relative number of acid sites strong enough to catalyze ring contraction. Strength variation within these acid sites can be estimated by comparing selectivity patterns accompanying ring contraction. Although among the least thermodynamically stable isomers, ECP is the initial MCH ring-contraction product formed in measurable quantities and is the majority product over lower acid strength catalysts at conversions less than 10%. At higher reaction temperatures and MCH conversions greater than 50% an equilibrium distribution of DMCP isomers is approached over higher acid strength catalysts. The equilibrium concentration of ECP remains between 8 and 11% over the temperature range employed (473−613 K). Figure 5 illustrates the combined effect of acid strength and conversion level on ECP selectivity.

At lower conversions over a weak to moderate acid strength Pt/SAPO-11 catalyst ECP is the predominate product. As conversion continues to rise, selectivity to ECP decreases with increasing formation of the more thermodynamically favored DMCP isomers. Over the higher acid strength Pt/USY(Si/Al = 5.1) catalyst, ECP is initially formed well above its equilibrium level, however, the DMCP isomers predominate the product mix. At higher MCH conversion levels product distributions trend toward equilibrium values. Comparison at 10% MCH conversion clearly shows that the lower acid strength Pt/SAPO catalyst exhibits an ECP selectivity of 55% while the ECP selectivity shown by the higher acid strength Pt/USY (5.1) catalyst is much lower (30%). High ECP selectivities measured at 10−20% MCH conversion, indicating weak to moderate acid strengths, are

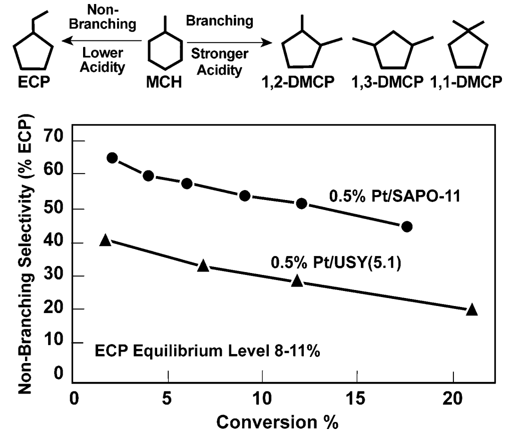

Figure 5. Branching patterns of MCH ring-contraction products reflect differences in acid site strength.

TABLE 4: MCH Conversion Activities are Responsive to Zeolite Framework to Si/Al Ratios

catalyst[a]	Si/Al	wt % @ 593 K[b] conv.	RC	cracking	ECP selectivity[c] @10% conv.
USY	66	47.3	46.6	0.71	54
USY	171	9.6	9.5	0.03	56
ZSM-5	12	37.4	30.6	6.3	34
ZSM-5	69	3.8	3.4	0.4	36
EU-1	18	59.7	49.7	9.8	30
EU-1	35	26.7	23.7	2.9	29
		equilibrium value			*8−11*

[a] Catalysts contain 0.5 wt % Pt. [b] Conditions: 473−613 K, 1475 kPa, WHSV = 31, H_2/MCH = 5.0. [c] Increasing % ECP values indicate decreasing acid strengths.

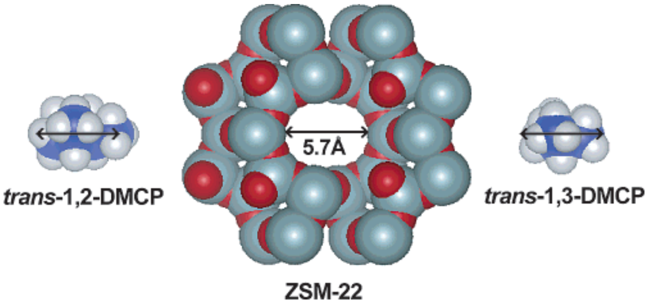

Figure 6. Dimethylcyclopentanes are appropriately sized to detect small porosity differences in 10-ring zeolites and microporous materials. While *trans*-1,3-DMCP can pass through the 5.7-Å channel opening of ZSM-22, *trans*-1,2-DMCP will experience a tighter squeeze.

TABLE 5: MCH Conversion Selectivites Reveal Porosity Differences Among Amorphous and Crystalline Solid Acids

catalyst[a]	Si/Al	pore size (Å)	wt % @ 593 K[b] conv.	RC	cracking	1,2-DMCP/ 1,3-DMCP[c] @ 593 K
USY	33	7.4 × 7.4	14.2	14.1	0.04	2.21
MOR	167	7.0 × 6.5	10.0	9.9	0.04	2.29
Beta	71	7.6 × 6.4	60.9	59.4	1.3	1.23
SAPO-11	0.05	6.3 × 3.9	8.2	8.1	0.1	0.34
ZSM-22	27	5.7 × 4.4	19.2	18.2	0.7	0.16
ZSM-5	110	5.6 × 5.3	21.1	21.0	0.1	0.02
ZSM-23	49	5.2 × 4.5	13.1	12.8	0.2	0.51
CLINO	5.2	7.6 × 3.0	6.1	5.9	0.1	1.94
$SiO_2-Al_2O_3$			15.8	15.7	0.05	2.16
ZSM-22/ $SiO_2-Al_2O_3$[d]			18.2	18.1	0.1	1.15
		equilibrium value				*1.8−1.9*

[a] Catalysts contain 0.5 wt % Pt. [b] Conditions: 473-613K, 1475kPa, WHSV = 31, H_2/MCH = 5.0. [c] Increasing trans-1,2DMCP/trans-1,3DMCP ratios suggest decreasing in-pore constraint. [d] 50/50 wt % mixture.

observed for amorphous $SiO_2-Al_2O_3$, halided-Al_2O_3, highly dealuminated USY, ZSM-22, and microporous materials such as SAPO-11. Lower ECP selectivities at 10−20% MCH conversion, which reflect a closer approach to an equilibrium isomer distribution, are exhibited by higher acid strength zeolitic materials such as ZSM-5, low Si/Al USY, mordenite, EU-1, and Beta.

3.4. MCH Conversion Activities are Responsive to Zeolite Framework Si/Al Ratios. The effect of framework Si/Al ratio upon the MCH conversion patterns of three representative zeolites, namely USY, ZSM-5 and EU-1, is summarized in Table 4. As would be expected, increasing Si/Al ratios by lowering the concentration of framework Al species (proportionally lowers acidic hydroxyl content) substantially reduces both ring-contraction and acid cracking activities for all three zeolites. ECP selectivity remained essentially constant for each zeolite regardless of the extent of dealumination. This finding strongly suggests that for the moderately to highly dealuminated zeolites compared here the relative strength of acid sites present in each individual zeolite is not appreciably altered upon additional Al removal.[15] It is possible that more aluminum-rich USY and EU-1 zeolites (Si/Al ratios < 10), which would have an increased number of nearest neighbor aluminum interactions, might exhibit modified ECP selectivities indicating, thereby, changes in acid strength. Based upon the ECP selectivities at 10% conversion, the relative acid strengths of the three zeolites listed in Table 4 decrease in the order EU-1 > ZSM-5 > USY.

3.5. MCH Conversion Selectivities Detect Differences in Solid Acid Porosities. The *trans*-1,2-DMCP/*trans*-1,3-DMCP product selectivity ratio was found to be highly dependent upon the pore size of a wide range of zeolitic and microporous solid acids. The basis for this pore size dependency can for the most part be accounted for by considering the space-filling model using van der Waals' radii for a ZSM-22 zeolite shown in Figure 6. While the smaller *trans*-1,3-DMCP isomer formed within the channels of ZSM-22 should readily exit through the 5.7-Å channel opening of ZSM-22, the larger *trans*-1,2-DMCP isomer which is also produced in the channels of the zeolite will experience a tighter squeeze which will likely hinder its egress from the 10-ring ZSM-22 crystal. Highly constraining 10-ring zeolites and 10-ring microcrystalline materials such as SAPO-11 consistently display *trans*-1,2-DMCP/*trans*-1,3-DMCP ratios of 0.5 or less. Larger pore size 12-ring zeolites and amorphous solid acids exhibit values ranging from 1.2 to 2.3 for this ratio. The *trans*-1,2-DMCP/*trans*-1,3-DMCP ratios for a number of crystalline 10- and 12-ring zeolites and microporous materials and an amorphous $SiO_2-Al_2O_3$ catalyst are compared in Table 5. An amorphous $SiO_2-Al_2O_3$ solid acid exhibits a *trans*-1,2-DMCP/*trans*-1,3-DMCP ratio of about 2.2 which is close to the equilibrium value of 1.8−1.9. This close approach to equilibrium suggests that the surface of amorphous $SiO_2-Al_2O_3$ does not restrict the transport of the various DMCP isomers. USY and mordenite zeolites displayed *trans*-1,2-DMCP/*trans*-1,3-DMCP ratios of 2.2 and 2.3, respectively, indicating that these large-pore, 12-ring zeolites, like the open structure of amorphous $SiO_2-Al_2O_3$, do not impede the generation of equilibrium quantities of the four DMCP isomers. The 12-ring Beta zeolite, which has a pore size similar to those of USY and mordinite, exhibited a substantially lower *trans*-1,2-DMCP/*trans*-1,3-DMCP ratio (1.2) indicating a greater degree of in-channel or pore mouth constraint. Markedly smaller *trans*-1,2-DMCP/*trans*-1,3-DMCP ratios, typically 0.5 or less, are observed for 10-ring zeolitic and microporous solid acids. For a given

TABLE 6: MCH Conversion Selectivity Patterns Readily Reflect Changes in the Crystallite Size of Zeolites and Microporous Materials

			wt % @ 593 K[b]			1,2-DMCP/ 1,3-DMCP[c]
catalyst[a]	Si/Al	crystallite size (μ)	conv.	RC	cracking	@ 593 K
SAPO-11	0.05	0.1−1.0	8.2	8.1	0.1	0.34
SAPO-11	0.05	0.01−0.2	20.0	19.9	0.02	1.33
ZSM-1	13	2.0	14.1	10.1	3.9	0.19
ZSM-1	15	0.01−0.2	43.2	22.2	20.8	0.45
		equilibrium value				*1.8−1.9*

[a] Catalysts contain 0.5 wt % Pt. [b] Conditions: 473−613 K, 1475 kPa, WHSV = 31, H_2/MCH = 5.0. [c] Increasing trans-1,2DMCP/trans-1,3DMCP ratios suggest decreasing in-pore constraint.

10-ring material it is possible to modify its *trans*-1,2-DMCP/*trans*-1,3-DMCP ratio by a variety of selectivation treatments.[16] The extremely low isomer ratio of 0.02 shown by ZSM-5 is not consistent with its pore size which is similar to those of both ZSM-22 and ZSM-23. It is possible that ZSM-5 (and perhaps Beta as well) exhibits a lower *trans*-1,2-DMCP/*trans*-1,3-DMCP ratio than expected as the result of the formation of an in-channel and/or pore mouth constricting carbon overlayer that rapidly forms on this zeolite during the initial on oil line out period.[17] In the case of a CLINO-based catalyst the extreme elliptical nature of the pore mouth of this 10-ring zeolite is so restrictive that MCH conversion occurs primarily on the outer surface, this significantly reduces conversion and produces a *trans*-1,2-DMCP/*trans*-1,3-DMCP ratio value typical of a non-constraining, open surface. Finally, a 50/50 by weight mixture of ZSM-22 with an amorphous $SiO_2-Al_2O_3$ demonstrates a *trans*-1,2-DMCP/*trans*-1,3-DMCP ratio that is the average value of the two components. In cases where the constituent parts have largely different activities the composite isomer ratio closely scales with relative activities. The ability to monitor subtle changes in the relative amounts of in-channel and outer surface activities of neat as well as bound 10- and 12-ring zeolites and microporous materials is an important and highly informative feature of the MCH ring-contraction probe reaction.

3.6. Crystallite Size Modifications in Zeolites and Microporous Materials are Readily Reflected in MCH Conversion Selectivity Patterns. As shown in Table 6, reducing crystallite size by an order of magnitude results in 2−3-fold activity enhancements for both SAPO-11 and ZSM-5.

In the case of ZSM-5 acid site cracking yield over the smaller crystal size material is also substantially increased relative to that of ring-contraction. Additionally, as indicated by increased *trans*-1,2-DMCP/*trans*-1,3-DMCP isomer ratios, the extent of exterior surface versus in-channel activity for both SAPO-11 and ZSM-5 is markedly enhanced by decreasing crystallite size. Thus, modifying the crystallite size of 10-ring zeolites and microporous materials can significantly alter the relative proportion of in-channel acid site catalysis.

4. Conclusion

Under well-defined test conditions, MCH ring-contraction has been established not only as a reliable measure of the relative number and relative strength of acid sites for both amorphous and crystalline solid acids, but it has utility in assessing shape selectivity differences among a wide range of 10-ring and 12-ring zeolites and microporous materials.

References and Notes

(1) Rabo, J. A. *Catal. Today* **1994**, *22*, 201.

(2) Hoelderich, W. F.; Heitmann, G. *Catal. Today* **1997**, *38*, 227.

(3) Schulz, H. F.; Weitkamp, J. H. *Ind. Eng. Chem. Prod. Res. Dev.* **1972**, *11*, 46.

(4) Alvarez, F.; Montes, A.; Perot, G.; Guisnet, M. In *Zeolites: Facts, Figures, Future*; Jacobs, P. A., vanSanten, R. A., Eds.; Elsevier: Amsterdam, 1989; p 1367.

(5) Brouwer, D. M.; Hogeveen, H. In *Progress in Physical Organic Chemistry*; Streitwieser, A., Jr., Taft, R. W., Eds.; Wiley-Interscience: New York, 1972; Vol. 9, p 179.

(6) Weitkamp, J.; Jacobs, P. A.; Ernst, S. In *Structure and Reactivity of Modified Zeolites*; Jacobs, P. A, Jaeger, N. I., Jiru, P., Schulz-Ekloff, G., Kazansky, V. B., Eds.; Elsevier: Amsterdam, 1984; p 279.

(7) Weisz, P. B. *Pure Appl. Chem.* **1980**, 52, 2091.

(8) Meir, W. M.; Olson, D. H. *Atlas of Zeolite Structure Types;* Butterworth-Heineman: Boston, 1992.

(9) McVicker, G. B.; Baker, R. T. K.; Garten, R. L.; Kugler, E. L. *J. Catal.* **1980**, *65*, 207.

(10) Beyerlein, R. A.; McVicker, G. B.; Yacullo, L. N.; Ziemiak, J. J. *J. Phys. Chem.* **1988**, *92*, 1967.

(11) McVicker, G. B.; Touvelle, M. S.; Hudson, G. W.; Vaughan, D. E. W.; Daage, M.; Hantzer, S.; Klein, D. P.; Ellis, E. S.; Cook, B. R.; Feeley, O. C.; Baumgartner, J. E. U.S. Patent 5,763,731, June 9, 1998.

(12) Weisz, P. B. *Chemtech* **1973**, 498.

(13) Ghosh, A. K.; Kydd, A. *Catal. Rev.- Sci. Eng.* **1985**, *27*, 539.

(14) Stull, D. R.; Westrum, E. F.; Sinke, G. C. *The Chemical Thermodynamics of Organic Compounds*; Wiley: New York, 1969.

(15) Haag, W. O.; Lago, R. M.; Weisz, P. B. *Nature (London)* **1984**, *309*, 589.

(16) Halgeri, A. B.; Das, J. *Catal. Today* **2002**, *73*, 65.

(17) Ashton, A. G.; Batmanian, S.; Dwyer, J.; Elliott, I. S.; Fitch, F. R. *J. Mol. Catal.* **1986**, *34*, 73.